Published in final edited form as:
Pflugers Arch. 2015 January ; 467(1): 15–25. doi:10.1007/s00424-014-1535-x.

MscL: channeling membrane tension

Troy A. Walton[1], **Chinenye A. Idigo**[1], **Nadia Herrera**[1], and **Douglas C. Rees**[*,1,2]

[1]Division of Chemistry and Chemical Engineering, California Institute of Technology, Pasadena, CA 91125

[2]Howard Hughes Medical Institute California Institute of Technology, Pasadena, CA 91125

Abstract

Mechanosensitive channels are integral components for the response of bacteria to osmotic shock. The mechanosensitive channel of large conductance (MscL) responds to extreme turgor pressure increase that would otherwise lyse the cellular membrane. MscL has been studied as a model mechanosensitive channel using both structural and functional approaches. We will summarize the structural data and discuss outstanding questions surrounding the gating mechanism of this homo-oligomeric channel that has ~3 nS conductance. Specifically we will explore: 1) the variability in oligomeric state that has been observed, 2) the open pore size measurements, and 3) the role of the C-terminal coiled coil domain for channel function. The oligomeric state of MscL has been characterized using various techniques, with a pentamer being the predominant form, however the presence of mixtures of oligomers in the membrane is still uncertain. In the absence of structural data for the open state of MscL, the diameter of the open state pore has been estimated by several different approaches, leading to a current estimate between 25 and 30 Å. While the C-terminal domain is highly conserved among MscL homologues, it is not required for activity *in vivo* or *in vitro*. This domain is likely to remain intact during the gating transition and perform a filtering function that retains valuable osmolytes in the cytosol. Overall, studies of MscL have provided significant insight to the field, and serve as a paradigm for the analysis of nonhomologous, eukaryotic mechanosensitive channel proteins.

Introduction

Mechanosensors are a ubiquitous class of biomolecules that play key roles in transducing mechanical force into signals for regulation of proper development and survival of living organisms [24]. Mechanosensing channels are implicated in many functions such as the senses of hearing and touch in animals, gravitropism in plants, and osmoregulation in bacteria. As examples, the Piezo channel family is mechanically activated, cation selective, and exemplifies mechanotransduction in vertebrates and invertebrates [11,12]. The MscS-like (MSL) family of proteins in the plant *Arabidopsis thaliana* helps maintain the correct shape and size of plastids, which are organelles involved in photosynthesis and gravity sensing [21]. Under hypo-osmotic stress, bacteria are able to alleviate turgor pressure

[*]corresponding author; dcrees@caltech.edu, (626) 395-8393 (phone), (626) 744-9524 (fax).

through mechanosensitive channels that gate directly in response to tension in the membrane lipid bilayer (Fig. 1, [8,43]).

Stretch-activated bacterial ion channels were discovered by Kung's group using patch clamp experiments on *Escherichia coli* giant spheroplasts [30]. As bacteria contain a variety of different channels (Table 1), the crucial breakthrough was the identification by C. Kung's group of channels that conducted only when tension was applied to the membrane by the application of suction to the patch pipette [30]. The first channel to be discovered, later identified as the mechanosensitive channel of small conductance (MscS) [27,44], demonstrated a single channel conductance of ∼1 nS and showed both pressure and voltage dependence, and selectivity for anions. When subjected to even stronger suction, patches excised from *E. coli* giant spheroplasts showed activation of another ion channel with ∼3 nS conductance [43]. This channel was identified as the mechanosensitive channel of large conductance (MscL). MscL shows no ion selectivity and is localized in the inner membrane [6,20,44]. Experiments on purified MscL reconstituted into azolectin liposomes indicate that MscL is gated solely by tension in the membrane lipid bilayer. The tension required to gate MscL is near the lytic limit of the membrane, ∼10-12 mN m^{-1} [25]. In osmotic down shock assays, *mscS/mscL* double knockout cells have poor survivability [27]. These findings make it clear that a critical function of mechanosensitive channels is to serve as emergency release valves in bacteria. The discovery of such a simple yet robust system provides an ideal model to study the mechanism of mechanosensation and the structural dynamics of channel gating.

A key development in establishing the molecular basis of mechanosensation was the identification by Kung's group of the gene for *E. coli* MscL, which encoded a 136 amino acid polypeptide [44]. Given the small subunit size, the large conductance of MscL and results of preliminary experiments on a size exclusion column where MscL elutes at a volume consistent with a molecular mass of roughly 70 kDa, it was postulated that the active form of MscL is a homo-oligomer [44]. MscL has since been identified in numerous bacterial species [33,39]. The best studied MscL orthologues are from *E. coli*, *Staphylococcus aureus*, and *Mycobacterium tuberculosis* (EcMscL, SaMscL, MtMscL, respectively); these channels contain 136, 120, and 151 residues, respectively, and the pairwise percent sequence identity between these proteins are EcMscL - MtMscL (37%), SaMscL - MtMscL (40%), and EcMscL - SaMscL (51%).

To date there are three crystal structures of MscL; MtMscL [10,40], a C-terminal truncation of SaMscL (SaMscL(CΔ26)) [28], and the EcMscL C-terminal domain (EcMscL-CTD) [49] (Fig. 2). The structure of MtMscL determined at 3.5 Å resolution established the basic subunit architecture and revealed a pentameric channel with the subunits surrounding a central pore (Figs. 2A and 2E). In agreement with hydropathy predictions and other biochemical analyses [6,44], the MscL subunit was found to contain two transmembrane (TM) helices. The first 12 amino acids of the N-terminus are located on the cytoplasmic side of the membrane and form an amphipathic α-helix followed by the first transmembrane helix, (TM1; residues 13-47; Fig. 2A, magenta), that crosses the membrane and lines the permeation pathway of the channel. Residues 48-68 are located on the periplasmic side of the membrane and form an extended loop with two antiparallel β-sheets (Fig. 2E, light blue). A second transmembrane α-helix, (TM2; residues 69-101, Fig. 2A, orange) traverses the

membrane again, from the periplasm towards the cytoplasm, and flanks the exterior of the channel. The C-terminal domain (Fig. 2A, light cyan) consists of a short loop (residues 102-105), followed by a left-handed coiled coil formed by α-helical residues 106-125. Residues 126-151 were not resolved and are presumably disordered in the crystal. TM1 forms the core of a complex network of interactions between subunits in the transmembrane region. The TM1 of one subunit interacts with TM1s from two adjacent subunits with a crossing angle of approximately −41°. TM1 also interacts with TM2 from the same subunit with a crossing angle of nearly 134°, and another TM2 from an adjacent subunit with a nearly antiparallel crossing angle of approximately −175°. In addition, the N-terminal α-helix of one subunit inserts between the TMs of an adjacent subunit at the cytoplasmic membrane interface. The narrowest part of the permeation pathway of the channel is largely hydrophobic, particularly at the constriction point, formed by the side chains of Ile 17 and Val 21, where the pore diameter is estimated to be between 2-3 Å. Theoretical models predict that a hydrophobic pore of ∼9 Å diameter is required to conduct water and ∼13 Å to conduct hydrated ions [4]. Therefore the conformation of the MtMscL structure is designated as a closed or non-conducting state.

The SaMscL(CΔ26) crystal structure was reported at 3.8 Å resolution (Figs. 2B and 2F) [28]. In contrast to the MtMscL structure, SaMscL(CΔ26) adopted a tetrameric oligomeric state with a shorter, widened conformation. As compared to the MtMscL structure, the N-terminal region (residues 1-12) and periplasmic loop (residues 48-64, Figs. 2B and 2F, blue) of SaMscL(CΔ26), while ordered, do not adopt regular secondary structures. The first transmembrane helix (residues 13-47, Fig. 2B, magenta) has the same number of residues as TM1 in MtMscL. TM2 (residues 65-90, Fig. 2B, orange) and the periplasmic loop of SaMscL(CΔ26) are seven and four residues shorter respectively than those of MtMscL. In SaMscL(CΔ26), TM1 also lines the permeation pathway, but relative to MtMscL, it adopts a larger tilt angle with respect to the pore axis. As in the MtMscL structure, TM1 of one subunit interacts with TM1s from two adjacent subunits, but with an increased crossing angle of approximately −63°. TM1 still interacts with TM2 from the same subunit with a more perpendicular crossing angle (∼111°), and another TM2 from an adjacent subunit with a crossing angle of approximately −191°. The pore diameter at the construction point, Val 21, is expanded to ∼6 Å. This pore size is still not large enough to allow passage of water or hydrated ions; therefore, this structure is designated as a non-conducting expanded intermediate state.

The structure of EcMscL-CTD spanning residues 108-136, was determined at 1.45 Å resolution (Fig. 2D) [49]. It revealed a pentameric α-helical coiled coil (residues 116-136) and an irregular extended region (residues 108-115). The EcMscL-CTD has almost three heptad repeats and shows the characteristic knob into hole packing of hydrophobic residues at periodic intervals expected for a coiled coil [49]. This arrangement is similar to the MtMscL-CTD and to other coiled coils, such as the cartilage oligomeric matrix protein (COMP) [29]. The observed structure is in agreement with an earlier model proposed by Sukharev and Guy for this region [1]. These structural studies on three different homologues of MscL have highlighted the basic features of MscL architecture; however, functional studies have almost exclusively explored the *E. coli* homologue.

In the 20 years after the identification of the gene for EcMscL by Kung and coworkers [44], extensive functional and structural studies have contributed to a deeper understanding of mechanosensation at the molecular level. Several key issues concerning the molecular mechanism of MscL remain unresolved, of which three are highlighted in this review (see Fig. 1).

1. The crystal structures of MtMscL, SaMscL(CΔ26), and EcMscL-CTD have raised questions about the physiological significance (if any) of the variability in oligomeric state observed for MscL. Varied oligomeric states of MscL generate uncertainty regarding effects of detergent solubilization (a common practice for *in vitro* membrane protein experiments) and the conformation of the channel *in vivo*.
2. While the open state has been modeled extensively by experimental and theoretical calculations, a crystal structure of the open state of MscL has not yet been determined. Without an authentic open state crystal structure, the dimensions of the permeation pathway responsible for the large conductance have been measured by indirect methods.
3. The conformation, helical bundle or random coil, of the CTD in the open channel state has been uncertain. The role of this domain as a molecular size filter and/or a restraint in gating energetics may be dependent on the conformational flexibility of this region.

In this review the literature on these topics will be discussed and future directions for research will be explored.

Oligomeric State

To achieve nS conductance from a protein of only 136 residues, EcMscL was postulated to form a homo-oligomer when it was first identified [44]. Determination of the correct oligomeric state of MscL is critical to inform estimations for pore diameter and gating mechanism. There have been three major waves of publications addressing the oligomeric state of MscL, coinciding with i) isolation of the EcMscL gene, ii) publication of the pentameric crystal structure of MtMscL, and iii) publication of the tetrameric structure of SaMscL(CΔ26). The oligomeric state of MscL has been studied using various biochemical and biophysical techniques, which include covalent crosslinking [1,6,10,15,20,23,46,52,53], tandem subunit fusions [6,16,46], 2-D electron crystallography [37], atomic force microscopy (AFM) [34], X-ray crystallography [10,28,40,49], analytical ultra centrifugation (AUC) [15,46], size exclusion chromatography coupled to multiangle laser light scattering (SEC-MALS) [15,17], and oligomer characterization by addition of mass (OCAM) [17]. Researchers have studied the oligomeric state of various wild type and mutant MscL constructs *in vivo* and *in vitro*. After nearly 20 years of study, the reported oligomeric state of MscL has ranged from monomer [20] to hexamer [6] (Table 2). In this section, the results of these studies, along with the strengths and weaknesses of different techniques used will be discussed. We will briefly touch on factors, such as lipid/detergent environment and sequence space that influence the variability of MscL oligomeric state.

Perhaps the most labor intensive method to determine the oligomeric state of MscL has been structural biology. X-ray crystallography, 2-D electron microscopy and atomic force microscopy (AFM) have all been used to image MscL with various results [10,28,34,37,40,49]. The highest resolution structures can be resolved by X-ray crystallography, and to date there are three crystal structures of MscL homologs or subdomains [10,28,40,49]. X-ray crystallography is a low-throughput technique because the limiting factors in X-ray structure determination of MscL are crystal formation and crystal quality. MscL is readily overexpressed in *E. coli* and purification gives relatively high protein yields. Nevertheless, as for most membrane proteins, MscL is recalcitrant to crystallization; and even when crystals appear, they are typically of poor diffraction quality. Chang *et al.* screened 9 MscL homologs, 20 detergents and over 24,000 crystal conditions before they were able to resolve the structure of MtMscL. Liu *et al.* determined a structure of truncated SaMscL after several years of work on full length EcMscL and SaMscL. Furthermore, Walton and Rees crystallized the soluble C-terminal domain of EcMscL to provide the first structural information for the *E. coli* homologue (while crystals of full length EcMscL have been obtained for nearly 20 years, their resolution has never exceeded ∼8 Å). These structures revealed MtMscL as a pentamer (Figs. 2A and 2E), SaMscL(CΔ26) as a tetramer (Figs. 2B and 2F) and EcMscL-CTD as a pentamer (Fig. 2D). The origins of this variability in oligomeric state has not been established, and may reflect the intrinsic preferences of the protein sequence, as well as external factors such as the use of detergents, or the selective crystallization of a particular oligomeric state. It should be noted, however, that, the oligomeric state of detergent solubilized MtMscL and SaMscL(CΔ26) observed crystallographically have been confirmed with other methods [17].

2-D electron crystallography was used to resolve an EcMscL structure to a resolution of 15 Å. This study suggested that EcMscL is a hexamer [37]. Detergent purified EcMscL was reconstituted into *E. coli* lipid liposomes at high protein to lipid ratios to form vesicular 2-D crystals. Negatively stained single layer 2-D crystals were imaged, and the 14 best images were processed. Two types of analysis, a filtered image without symmetry applied, and filtered images with a six-fold symmetry plane group applied, produced projection maps with apparent six-fold symmetry. The EcMscL molecules were visualized as hexagonal particles with a central depression. This was interpreted to be six EcMscL subunits in a ring lining a pore. At the resolution of the study, however, it is difficult to see such features with high certainty. AFM studies were performed on *Salmonella typhimurium* MscL (StMscL) immobilized on organic monolayers that allowed for experimental control of protein tension and adhesion [34]. These studies show that on a surface with a tension between 20-30 mN m^{-1}, StMscL is present in the form of nanoscale entities with a diameter of 4-5 nm, interpreted as a pentameric structure. The dimensions of the AFM probe, and the influence of the probe on the lateral dimensions recorded for subject proteins, likely limit the resolution of these studies.

Historically, covalent cross-linking has been the most popular technique for determining the oligomeric state of MscL, as it is relatively simple, fast, and inexpensive. Cross-linking, however, has generated the most varied and ambiguous results (Table 2), due to differences in cross-linker specificity, length, concentration, and reaction environment. Several studies

have used non-specific cross-linking agents, such as disuccinimidyl suberate (DSS), which reacts with primary amine groups. Studies using DSS have given different results, even with comparable protocols. An early cross-linking study by Blount *et al.* used DSS to cross-link purified EcMscL solubilized in β-octylglucoside [48]. The products of the reactions were separated by SDS-PAGE and visualized via silver staining. Six distinct bands were observed, indicating EcMscL is hexameric [6]. Similar results were observed when purified membrane fractions were cross-linked, and products were visualized via western blot.

Subsequently, Sukharev *et al.* performed cross-linking experiments with OG purified EcMscL, using variable concentrations of DSS [46]. At lower concentrations of DSS, there were over eight distinct bands on an SDS-PAGE gel, visualized with Coomassie Blue dye. At higher concentrations of DSS, both the higher and lower molecular weight bands disappeared, leaving three prominent bands with the most intense migrating at a molecular weight consistent with pentameric MscL. Based on these results and those of similar experiments using other crosslinking agents, EcMscL oligomeric state was interpreted as pentameric. Since DSS has a relatively long linker length (11 Å), the higher molecular weight bands were attributed to intercomplex crosslinking. It should be noted, however, that these studies used slightly different crosslinking protocols.

To address some of the issues of non-specific crosslinking agents and detergent effects, several studies have used a disulfide trapping strategy to crosslink MscL in membranes [1,15,23,41]. Both wild-type SaMscL and EcMscL lack cysteine residues, making site-specific cysteine mutants relatively simple to generate. The double cysteine mutant, SaMscL L10C/M91C, has intracellular cysteine residues in the N-terminal and TM2 regions of SaMscL. Experiments conducted in whole cells require an oxidizing agent, such as copper phenanthroline to catalyze disulfide bond formation in the cytosol following osmotic shock to activate the channel. This process allows the copper phenanthroline complex to enter the cell directly through the MscL pore, since it will not otherwise diffuse across the membrane. The products of the reaction are then detergent extracted in non-reducing SDS sample buffer, without quenching the reaction, and visualized by western blot. Based on such studies, Dorwart *et al.* suggest that SaMscL is pentameric when overexpressed in the *E. coli* membrane.

In general, crosslinking experiments are interpreted in a qualitative fashion, which can be problematic for the unambiguous determination of the oligomeric state of proteins. Reaction conditions that produce a ladder of bands for easy ‘counting’ of subunits may lead to incomplete reactions and possibly bands that represent concatamers of cross-linked subunits [2]. Furthermore, reaction conditions that produce fewer bands (or a single band) can lead to products that migrate at molecular weights inconsistent with the true molecular weight of the complex, due to concatamers as well as intramolecular cross-links. A particularly challenging situation occurs when mixtures of different oligomeric states are present; the series of bands for the smaller oligomer(s) will be a subset of the ladder for the largest oligomer. Due to these intrinsic difficulties with cross-linking, alternatives methods have been employed to determine the oligomeric state of MscL.

Genetic fusion of individual MscL subunits, followed by electrophysiology and crosslinking also led to the conclusion that MscL is hexameric [6]. In these experiments, tandem fusions of MscL subunits generate functional channels in the bacterial membrane, as well as when reconstituted into liposomes. This observation of channels, presumably formed by an even number of subunits, combined with cross-linking experiments provided additional evidence for the hexameric form of EcMscL. A subsequent study using a similar approach, but including triple subunit fusions also produced functional channels [46]. In this study, the observation that double subunit fusion constructs form larger channels by SEC than monomeric constructs implied that the wild type monomeric protein assembles into a smaller pentameric channel [46]. Poolman and co-workers later repeated this genetic fusion approach with additional subunits fused together, forming up to six in a single protein chain. Interestingly, all constructs, from single to hexameric subunit fusions, produced functional channels [16]. Remarkably these fusions form functional channels with only one [6,46] or two [16] amino acid containing linkers between the C-terminus of one subunit and the N-terminus of the next. This arrangement appears to require that the structure of either the N-terminal helix or the C-terminal bundle will be perturbed if the fusions assemble into the same channel. Given that the N-terminus is more sensitive to modification than the C-terminus [7], we would expect the perturbation to be at the C-terminal bundle in cases where these fusions assemble into functional channels.

Mass separation techniques such as SEC-MALS and AUC have been used to study the detergent solubilized molecular weight of several MscL homologs [15,17,46]. Sedimentation equilibrium experiments of detergent solubilized EcMscL were unable to observe a single species due to protein aggregation in the detergent/lipid mixture analyzed [46]. The data obtained showed the presence of two or more species and was fit to a two non-interacting species model. Calculating the molecular weight of the EcMscL complex from the experimental reduced molecular mass requires the estimation of detergent mass contribution. Since the amount of detergent bound to each MscL complex is unknown, it is difficult to estimate the respective mass contributions of protein and detergent. Sukharev *et al.* concluded that MscL forms aggregates in OG and speculated that this may also be true in native membranes based on the observation that addition of lipids to the mixture did not ablate aggregation. Sedimentation equilibrium was also used to calculate the molecular mass of SaMscL [15]. The detergent C8E5 was chosen for solubilization, as it is neutrally buoyant in the experimental conditions. The data was fit to a single species model and the protein mass was calculated to be 71.2 kDa, which corresponds to a pentamer (72.2 kDa). Results from a sedimentation velocity experiment of SaMscL solubilized in LDAO led to a calculated protein mass of 62.5 kDa, which corresponds to a tetramer (57.8 kDa). This result is consistent with the oligomeric state observed in the SaMscL(CΔ26) structure. Detergent mass and buoyancy were accounted for with protein-free controls. SECMALS has the ability to separate aggregates from single channel protein detergent complexes, but uncertainty in determining the protein and detergent contributions to the scattering mass observed introduces error into the measurement. SEC-MALS has been used with limited success in measuring the molecular weight, and thus, oligomeric state of several MscL homologues. In our laboratory, we have observed good agreement between measured and theoretical pentameric molecular weight for most homologs tested; an exception is EcMscL, which is

consistently measured at ∼100 kDa, a mass more consistent with a hexameric oligomer [17]. If mixtures of oligomers exist in the detergent solubilized state, currently available SEC columns are not able to separate them.

In view of the challenges in determining the oligomeric state of membrane protein complexes, we developed a new method to the measure oligomeric state of multiprotein complexes. Oligomer characterization by addition of mass (OCAM) is capable of unambiguous measurement of the oligomeric state for any protein complex and also has the ability to detect mixtures of oligomers, if they exist [17]. OCAM counts protein subunits by selectively removing a mass tag fused to a protein subunit via a short peptide linker. Cleavage of each mass tag through a specific proteolytic site in the linker peptide reduces the total mass of the protein complex by an amount defined by the fused mass partner. Limited proteolysis and separation of the reaction products by size, via Blue Native PAGE, reveals a ladder of reaction products corresponding to the number of subunits present in the target complex plus one additional band for the completed reaction product. The pattern of bands may be used to distinguish the presence of a single homo-oligomer from a mixture of oligomeric states. Using this approach, we were able to determine the oligomeric state of several MscL homologs. Full length MtMscL and SaMscL are pentameric, while the CTD truncations are pentameric and pentamer/tetramer mixtures respectively. EcMscL is a mixture of hexamer and pentamer forms by OCAM. Unfortunately OCAM, as described above, does not address the *in vivo* oligomeric state because it requires detergent solubilized protein. There are also compatibility issues between certain detergents and BN-PAGE that limit the range of conditions accessible by OCAM, and the possibility that some oligomers may partially dissociate under the conditions used to run BN-PAGE experiments. Nevertheless, the results of our OCAM studies are consistent with the Xray crystallography for MtMscL and some of the cross linking results.

The cumulative data collected on the oligomeric state of MscL have added richness to the picture of MscL structural arrangement. These studies have revealed the variability of MscL oligomeric state and the effects of detergent and sequence diversity. There is currently, however, no method available that detects mixtures of oligomeric state in a membrane bound channel, which is an important technical development to solve in the future. Ultimately, characterization of the MscL oligomeric state will impact studies focused on estimating the pore size, and gating mechanism.

Pore Size

The conductance of MscL, ∼3 nS, is much larger than that of other channels found in bacteria [43,44]. For example, the KcsA potassium channel, arguably the best studied bacterial channel, has a conductance of ∼0.1 nS [26,38]. The relatively nonselective outer membrane porin OmpF has been measured with higher conductance, ∼0.3 nS, for a single 10 Å diameter pore of the trimeric protein [3,13]. The high conductance of MscL, therefore, suggests a very large open pore size. No crystal structure exists of the open state of MscL; nevertheless several other methods have been used to estimate the pore size of the MscL open state.

The first estimates of pore size for EcMscL used conductance measurements, coupled with calculations based on a conductance relationship discussed by Hille [22], to assess the pore diameter necessary to allow passage of ions sufficient to achieve the measured current [14]. These calculations assumed a channel of uniform length and radius in a solution of known resistivity. Assumptions were made for the channel length; since MscL resides in the inner membrane and it is estimated to require ∼28 amino acids in an α-helical conformation to cross the membrane, the overall length of the permeation pathway would be about 42 Å. With a conductance measured at 3.8 nS, Cruickshank *et al.* estimated the open pore diameter was also roughly 42 Å [14]. In the same study, the authors measured the passage of various sized poly-L-lysines (PLL) through the channel pore to achieve an alternate estimate of MscL pore diameter near 37 Å. These estimates were later improved by imaging the patch-clamp experiment to better measure the force on the channel from changes in patch curvature at different pressures [47]. These measurements were then used to calculate the change in cross sectional area upon gating, which led to better estimates of the total pore diameter in the open state. Again using the Hille model, a range of estimates for the open pore diameter were calculated between 27 and 35 Å for a pore length range from 20 to 50 Å, respectively. The Hille model is based on the assumption that the pore is a cylinder. Given the known structures of MscL where the pore is more conical or funnel shaped, these estimates are likely to include error from the assumption of a cylindrical pore. By calculating a range of pore lengths, however, Sukharev *et al.* account for the possibility that a given region of the MscL open pore is cylindrical in shape even if the shape through the complete distance across the membrane does not resemble a perfect cylinder [42].

Pore dimensions derived from geometric considerations have been refined by studies that observe the passage of molecules of known size through the open MscL channel. As noted above, polyamines, including various PLLs, were the first type of molecules used for such a measurement [14]. It was found that small polyamines such as cadaverine could readily pass through the pore. PLL_{19} (25 Å average diameter) did not reduce MscL channel conductance when added to the bath solution, while PLL_{46} (37 Å average diameter) did decrease the measured conductance. More recently, an elegant approach to the problem using Dual Color Fluorescence Burst Analysis (DCFBA) has been described using small proteins (with known structures), rather than polyamines, as size markers for passage through the pore [48]. In this method, MscL is reconstituted into liposome membranes containing a subpopulation of fluorescently labeled lipids, which encapsulate fluorescently labeled, water soluble, molecules. The fluorescence intensity of both molecules is measured as the liposomes diffuse through the observation volume of a microscope and the time correlation of the two signal intensities is calculated. If both fluorescent signals are highly correlated (unchanged after MscL opening), then the encapsulated molecules are likely to still be inside the liposome, whereas poorly correlated signals suggest that the encapsulated molecules have been released through the MscL pore. In these experiments, MscL opening is triggered by charge repulsion in the pore, which is achieved by modifying pore lining cysteine mutants of MscL with charged sulfhydryl modifying agents such as MTSET. In these experiments, molecules as large as 6.5 kDa (bovine pancreatic trypsin inhibitor) with dimensions 21 × 23 × 31 Å pass through MscL in the open state. These experiments were recently repeated on MscL channels that could be modified at the single subunit level rather than all subunits at

once as in previous experiments [32]. The results for the pore diameter of the completely open channel were unchanged; however, a partially gated channel (one labeled subunit) did display a smaller pore diameter estimated near 10 Å.

Open state structures of MscL have been proposed using a combination of disulfide crosslinking, electrophysiology, molecular dynamics (MD) [41], and electron paramagnetic resonance spectroscopy (EPR) [36]. Unfortunately, the initial crystallographic model for MtMscL (PDB: 1MSL) contained several registry errors that undoubtedly increased the difficulty in generating reliable *in silico* models. For the Sukharev-Guy models, experimental data from disulfide crosslinking and electrophysiology were used with MD simulations to determine potential open state models of MscL. Among several criteria applied to generate the models, the pore diameter was limited between 30 and 40 Å since this was the range previously reported in the literature. The final models produced from these experiments suggest an iris-like model of helix tilting and rearrangements to generate an open pore diameter of 36 Å (Figs. 2C and 2G). EPR experiments used by Perozo and co-workers to measure open state distances in MscL indicated a minimum pore diameter of 25 Å. To measure these distances using EPR, a family of single cysteine mutants was created for spin labeling that encompassed both the transmembrane helices (residues 14-43 and 72-96). EPR data was collected in different conditions that correspond to closed, intermediate, and open states; the latter was generated by the addition of lysophospholipids to the MscL-containing proteoliposomes. The data from these experiments was then used to create restraints for building a model of the MscL open state. Since data was collected only for the transmembrane helices, only these regions were modeled. The pore size calculated from this approach is reported as a minimum due to the loss of spin-spin interactions beyond ∼15 Å, coupled with the expected helix tilt required to satisfy the data at other positions in the modeled transmembrane regions.

AFM studies on StMscL immobilized in self-assembled organic monolayers have been used to directly image an open state. While under tension ranging between 30 and 60 mJ/m^2 [34], the signal for MscL corresponds to a protein with a height of 2.2-2.7 nm, and a pore of 11-15 nm. Though this approach has the advantage of being able to apply calibrated tensions to apparently gate MscL, these dimensions are significantly larger than that observed by any other method, and may reflect limitations arising from the effects of the AFM probe on the sample and the dimensions of the probe itself.

The most recent attempt to measure the pore diameter of the open MscL channel uses single molecule Förster resonance energy transfer (FRET) on tethered liposomes with MscL incorporated [51]. Various positions on TM1 and TM2 were labeled in a stochastic fashion with donor and acceptor dyes for FRET studies. Due to the nature of single molecule studies, Wang *et al.* were able to select appropriately dual labeled channels for analysis without interfering signal from channels labeled with more than a single donor and acceptor. A pore diameter of 28 Å was directly measured using the single molecule FRET approach and confirmed by using the distance constraints from FRET in MD simulations of an open channel.

The summary above has focused on data used to calculate the diameter of the open pore of MscL. Some of the estimates mentioned could be influenced by the conformational state of the C-terminal domain. Particularly, the molecular sieving experiments would seem to suggest that the EcMscL-CTD does not form a bundle in the open channel state.

C-terminal Domain

The role of the C-terminal domain of MscL in channel function has been extensively studied. Early studies (prior to the crystal structure determination) defined a region that can be deleted while still leaving a functional channel that can rescue cells from osmotic downshock [1,7]. While *in vivo* and *in vitro* studies of this region show that it is qualitatively unnecessary for MscL function, subtleties exist that point to an important function for the MscL-CTD. This region shows a high level of sequence conservation among MscL homologs [1]. The role of the CTD during gating depends on the final conformational state of this region. Data exists to support both a compact coiled coil in the closed state (as in the MtMscL structure), and a disordered coil in the open state [1,48,49,52].

The structural data available for MscL reveals two conformational states, a non-conducting “closed” state and a non-conducting “expanded intermediate” state [10,28,40]. One interpretation, from a structural point of view, suggests deletion of the MscL-CTD allows the expanded intermediate state to be trapped for crystallization, and thus, the CTD may disassociate during gating. The observation that SaMscL(CΔ26) has a longer open dwell time than the full-length channel also suggests a role for the CTD during gating. However, extensive *in vitro* studies of EcMscL provide additional data to the structural picture that are consistent with an intact CTD in the open high conductance state.

Several different studies agree that CTD deletions can generate a functional mechanosensitive channel able to both rescue bacteria *in vivo* and be reconstituted and respond to mechanical stimuli *in vitro* [1,7]. A precise definition of a role for the CTD has eluded random mutagenesis screens, which have not revealed a significant functional role for this region [31,33,35]. The maximum size of a CTD deletion that generates a functional channel in EcMscL is 27 amino acids, while a 33 amino acid deletion does not produce a functional channel [7]. It is not clear if the larger deletion produces a properly assembled, but non-functional channel, or whether this deletion causes folding defects that lead to channel degradation. A set of internal deletions to the linker between TM2 and the CTD coiled coil ranging from 2-5 amino acids (positions 110-112 or 110-115) still produces functional channels with reduced conductance compared to wild type protein [52]. This data further indicates that EcMscL-CTD is not very sensitive to deletions when assayed *in vitro.* The decreased conductance observed for these mutants suggests a decrease in the pore size. This decrease in pore size can only be caused if the CTD remains intact during the gating transition acting as an anchor point for the loop connecting TM2 and the CTD. If the CTD were to disassociate during the gating transition, then there would be nothing preventing the pore from opening to full size with a shortened linker between TM2 and the CTD.

The conformational state of MscL-CTD during the gating transition has been probed by measuring the channel activity with electrophysiology, while the CTD is cross-linked to

itself via engineered disulfide bonds. When cysteine residues are introduced into the CTD, the large conductance of MscL does not decrease under oxidizing conditions. This indicates that ions still flow through a pore of similar size to wild type even when the CTD is covalently cross-linked [1,52]. This behavior is seen whether the stimulus in the patch is, at saturation, measuring all channels in the patch, or at threshold, measuring only a subset of channels that start to open at low applied tensions. It is important to note that the disulfide cross-linking in these experiments is not quantitative and incompletely cross-linked channels could be measured under threshold stimulus. The experiments measuring current at saturation stimulus showed very little difference between oxidizing and reducing conditions, indicating that no additional channels were detected when cross-links were reversed. Data from disulfide cross-linking experiments are consistent with the interpretation that the EcMscL-CTD does not need to disassociate for proper channel gating. These experiments, however, have not been able to directly test the status of the EcMscL-CTD *in vivo* due to the reducing environment present in the bacterial cytosol.

Thermodynamic analysis of the EcMscL-CTD suggests that this domain is stable in the cytosol [49]. We have performed denaturation studies of the free CTD (29 residue peptide) monitored by CD spectroscopy to determine the energetics of unfolding for this domain. We observe a $\Delta G°$ value of $\sim$100 kJ/mol at standard state for this peptide. By calculating the effective concentration for EcMscL-CTD, we estimate the stability, in terms of melting temperature, of EcMscL-CTD in context of the full length channel present in the membrane to be well above 80° C. Our results indicate a stable, folded, EcMscL-CTD at the range of local concentration and temperature we would expect for intact EcMscL channels *in vivo* [49].

The presence of an intact MscL-CTD in the open state narrows the possible role for this domain. Effects on gating kinetics and open probability could be invoked to explain the function of this domain if it were to disassociate upon gating. Given the presence of ionic interactions that potentially destabilize the CTD when compared with similar coiled coil structures [9,18], it is tempting to speculate that these interactions act as a sensor of local osmotic strength that signals the appropriate time to close the channel after it has been triggered by hypo-osmotic shock [50]. Given that the CTD is more likely to remain intact during gating [1,49,52], it may serve a filtering role that prevents loss of important metabolites during hypo-osmotic shock. Opening of MscL will almost certainly depolarize the bacterial inner membrane and deplete significant energy stored in the proton motive force. Re-establishment of the proton gradient across the membrane will use ATP, a molecule small enough to easily pass through the MscL pore. If molecules such as ATP and glucose are depleted to a concentration below where the cell can recover, then the protective effect of MscL activity will be futile. Indeed, experiments on the EcMscL-CTD truncations have shown a greater loss of ATP when the CTD is truncated compared to wild type, although no difference from wild type survival rate was observed [1]. This ability to recover from shock even in absence of the CTD explains why this region has not been detected with random mutagenesis screens [31,35]. Thus, it is still not clear what selective pressure has maintained the presence and sequence conservation of MscL-CTD among bacterial homologs.

Conclusion

Our current understanding of MscL function is the product of the studies described above. The structures described add to a rich functional data set to paint a picture of a unique channel whose protective mechanism for bacteria subjected to hypo-osmotic shock is well established [1,27,28]. MscL has among the largest conductance measured for any channel, which suggests an oligomeric protein undergoing a large conformational change to adopt the open state. Two structures reveal snapshots of the protein likely along this conformational trajectory, but the endpoint of an open state channel has yet to be observed with high structural detail. An open state structure will enable measurements of the pore diameter and reveal the conformation of the CTD. Current estimates of the pore diameter converge on a value near 25-30 Å rather than the early estimates of 30-40 Å. There also appears to be convergence around the idea that the CTD remains intact during the gating transition. While a pentameric form may be the predominant species, whether or not there is a unique oligomeric state, or a mixture of oligomeric states, in the cell membrane has not been definitively established.

The observation of large molecules and small proteins passing through the open MscL pore appears to suggest that the CTD would be required to dis-assemble upon gating of the channel. Perhaps, but CTD dissociation may not be necessary if the gap between adjacent subunits at the linker region between TM2 and the CTD is at least as large as the open pore. In the absence of structural data for the open state, we can only speculate as to the size of this gap. Using the open state model reported by Sukharev and Guy, a distance of nearly 40 Å is measured between loops in this region (Fig. 2C) [42]. This is an even larger distance than the open pore in the same model. The same region in the MtMscL closed structure is occluded by the N-terminal helix of one subunit inserted between the TM2s of the two adjacent subunits. This orientation of the N-terminal helix in the closed state could be similar in the open state, thereby reducing the gap in the Sukharev and Guy-Model open state substantially, perhaps by half to ∼20 Å. Based on these estimations it is still possible to imagine small proteins and large molecules passing through the MscL pore even while the CTD remains intact. This speculation may reconcile what appear to be opposing sets of data, but still leaves open the question of why the CTD has remained part of the MscL channel across bacterial species.

The early observations of the small gene encoding MscL combined with the large conductance invoked the requirement for a homo-oligomer of MscL as the active membrane bound protein [6,19,44]. Several different measurements of the oligomeric state have been reported, and there is a general consensus around the pentameric form being predominant (Table 2). The presence of mixtures of MscL oligomers *in vivo*, whether having specific functional roles or serving as assembly intermediates, however, has not been definitively ruled out. Information contained in the sequence of MscL is a likely determinant of the oligomeric state, but no obvious motif is apparent when MtMscL is compared to SaMscL(CΔ26), which crystallizes as a pentamer and tetramer, respectively. The crossing angles observed for the transmembrane helices in different MscL structures can accommodate multiple oligomeric states, and unfortunately there is insufficient data at this

time to narrow down the regions of the protein that are ultimately responsible for a given oligomeric state.

The existence of large conductance, stretch activated channels at one point was controversial [5,30,45]; undoubtedly many more surprises await in deciphering the principles controlling the construction, operation and regulation of such large conductance channels across membranes. Harnessing MscL as a tool for drug delivery or as a target for antibiotic development will require a deep understanding of the gating mechanism in different homologues and in different lipid environments. Continued exploration of MscL structure and function among multiple homologues will add to the solid foundation of knowledge about this important model mechanosensitive channel.

Acknowledgments

We thank Chris Gandhi, Rob Phillips, Elizabeth Haswell and Ian Booth for stimulating discussions. N. Herrera is the recipient of a Gilliam graduate fellowship of the Howard Hughes Medical Institute, and C. Idigo received support from the US National Institutes of Health/National Research Service Award T32 GM07616. Research in the authors' lab was supported by US National Institutes of Health grant GM84211.

References

1. Anishkin A, Gendel V, Sharifi NA, Chiang CS, Shirinian L, Guy HR, Sukharev S. On the conformation of the COOH-terminal domain of the large mechanosensitive channel MscL. J Gen Physiol. 2003; 121:227–244. [PubMed: 12601086]
2. Azem A, Shaked I, Rosenbusch JP, Daniel E. Cross-linking of porin with glutardialdehyde: a test for the adequacy of premises of cross-linking theory. Biochim Biophys Acta. 1995; 1243:151–156. [PubMed: 7873557]
3. Basle A, Iyer R, Delcour AH. Subconductance states in OmpF gating. Biochim Biophys Acta. 2004; 1664:100–107. [PubMed: 15238263]
4. Beckstein O, Tai K, Sansom MS. Not ions alone: barriers to ion permeation in nanopores and channels. J Amer Chem Soc. 2004; 126:14694–14695. [PubMed: 15535674]
5. Berrier C, Coulombe A, Houssin C, Ghazi A. A patch-clamp study of ion channels of inner and outer membranes and of contact zones of *E. coli*, fused into giant liposomes. Pressure-activated channels are localized in the inner membrane. FEBS Lett. 1989; 259:27–32. [PubMed: 2480919]
6. Blount P, Sukharev SI, Moe PC, Nagle SK, Kung C. Towards an understanding of the structural and functional properties of MscL, a mechanosensitive channel in bacteria. Biol Cell. 1996; 87:1–8. [PubMed: 9004483]
7. Blount P, Sukharev SI, Schroeder MJ, Nagle SK, Kung C. Single residue substitutions that change the gating properties of a mechanosensitive channel in *Escherichia coli*. Proc Natl Acad Sci USA. 1996; 93:11652–11657. [PubMed: 8876191]
8. Booth IR, Louis P. Managing hypoosmotic stress: aquaporins and mechanosensitive channels in Escherichia coli. Curr Opin Microbiol. 1999; 2:166–169. [PubMed: 10322175]
9. Bosshard HR, Marti DN, Jelesarov I. Protein stabilization by salt bridges: concepts, experimental approaches and clarification of some misunderstandings. J Mol Recogn. 2004; 17:1–16.
10. Chang G, Spencer RH, Lee AT, Barclay MT, Rees DC. Structure of the MscL homolog from *Mycobacterium tuberculosis*: a gated mechanosensitive ion channel. Science. 1998; 282:2220–2226. [PubMed: 9856938]
11. Coste B, Mathur J, Schmidt M, Earley TJ, Ranade S, Petrus MJ, Dubin AE, Patapoutian A. Piezo1 and Piezo2 are essential components of distinct mechanically activated cation channels. Science. 2010; 330:55–60. [PubMed: 20813920]

12. Coste B, Xiao B, Santos JS, Syeda R, Grandl J, Spencer KS, Kim SE, Schmidt M, Mathur J, Dubin AE, Montal M, Patapoutian A. Piezo proteins are pore-forming subunits of mechanically activated channels. Nature. 2012; 483:176–181. [PubMed: 22343900]
13. Cowan SW, Schirmer T, Rummel G, Steiert M, Ghosh R, Pauptit RA, Jansonius JN, Rosenbusch JP. Crystal structures explain functional properties of two *E. coli* porins. Nature. 1992; 358:727–733. [PubMed: 1380671]
14. Cruickshank CC, Minchin RF, Le Dain AC, Martinac B. Estimation of the pore size of the large-conductance mechanosensitive ion channel of *Escherichia coli*. Biophys J. 1997; 73:1925–1931. [PubMed: 9336188]
15. Dorwart MR, Wray R, Brautigam CA, Jiang Y, Blount P. *S. aureus* MscL is a pentamer in vivo but of variable stoichiometries in vitro: implications for detergent-solubilized membrane proteins. PLoS biology. 2010; 8:e1000555. [PubMed: 21151884]
16. Folgering JH, Wolters JC, Poolman B. Engineering covalent oligomers of the mechanosensitive channel of large conductance from *Escherichia coli* with native conductance and gating characteristics. Protein Sci. 2005; 14:2947–2954. [PubMed: 16322576]
17. Gandhi CS, Walton TA, Rees DC. OCAM: a new tool for studying the oligomeric diversity of MscL channels. Protein Sci. 2011; 20:313–326. [PubMed: 21280123]
18. Gunasekar SK, Asnani M, Limbad C, Haghpanah JS, Hom W, Barra H, Nanda S, Lu M, Montclare JK. N-terminal aliphatic residues dictate the structure, stability, assembly, and small molecule binding of the coiled-coil region of cartilage oligomeric matrix protein. Biochemistry. 2009; 48:8559–8567. [PubMed: 19681593]
19. Hase CC, Le Dain AC, Martinac B. Purification and functional reconstitution of the recombinant large mechanosensitive ion channel (MscL) of *Escherichia coli*. J Biol Chem. 1995; 270:18329–18334. [PubMed: 7543101]
20. Hase CC, Minchin RF, Kloda A, Martinac B. Cross-linking studies and membrane localization and assembly of radiolabelled large mechanosensitive ion channel (MscL) of *Escherichia coli*. Biochem Biophys Res Comm. 1997; 232:777–782. [PubMed: 9126353]
21. Haswell ES, Meyerowitz EM. MscS-like proteins control plastid size and shape in Arabidopsis thaliana. Current biology. 2006; 16:1–11. [PubMed: 16401419]
22. Hille B. Pharmacological modifications of the sodium channels of frog nerve. J Gen Physiol. 1968; 51:199–219. [PubMed: 5641635]
23. Iscla I, Wray R, Blount P. The oligomeric state of the truncated mechanosensitive channel of large conductance shows no variance in vivo. Protein Sci. 2011; 20:1638–1642. [PubMed: 21739498]
24. Kung C. A possible unifying principle for mechanosensation. Nature. 2005; 436:647–654. [PubMed: 16079835]
25. Kung C, Martinac B, Sukharev S. Mechanosensitive channels in microbes. Ann Rev Microbiol. 2010; 64:313–329. [PubMed: 20825352]
26. LeMasurier M, Heginbotham L, Miller C. KcsA: it's a potassium channel. J Gen Physiol. 2001; 118:303–314. [PubMed: 11524460]
27. Levina N, Totemeyer S, Stokes NR, Louis P, Jones MA, Booth IR. Protection of *Escherichia coli* cells against extreme turgor by activation of MscS and MscL mechanosensitive channels: identification of genes required for MscS activity. EMBO journal. 1999; 18:1730–1737. [PubMed: 10202137]
28. Liu Z, Gandhi CS, Rees DC. Structure of a tetrameric MscL in an expanded intermediate state. Nature. 2009; 461:120–124. [PubMed: 19701184]
29. Malashkevich VN, Kammerer RA, Efimov VP, Schulthess T, Engel J. The crystal structure of a five-stranded coiled coil in COMP: a prototype ion channel? Science. 1996; 274:761–765. [PubMed: 8864111]
30. Martinac B, Buechner M, Delcour AH, Adler J, Kung C. Pressure-sensitive ion channel in *Escherichia coli*. Proc Natl Acad Sci USA. 1987; 84:2297–2301. [PubMed: 2436228]
31. Maurer JA, Dougherty DA. Generation and evaluation of a large mutational library from the Escherichia coli mechanosensitive channel of large conductance, MscL: implications for channel gating and evolutionary design. J Biol Chem. 2003; 278:21076–21082. [PubMed: 12670944]

32. Mika JT, Birkner JP, Poolman B, Kocer A. On the role of individual subunits in MscL gating: “all for one, one for all?”. FASEB J. 2013; 27:882–892. [PubMed: 23193173]
33. Moe PC, Blount P, Kung C. Functional and structural conservation in the mechanosensitive channel MscL implicates elements crucial for mechanosensation. Molecular microbiology. 1998; 28:583–592. [PubMed: 9632260]
34. Ornatska M, Jones SE, Naik RR, Stone MO, Tsukruk VV. Biomolecular stress-sensitive gauges: surface-mediated immobilization of mechanosensitive membrane protein. J Amer Chem Soc. 2003; 125:12722–12723. [PubMed: 14558816]
35. Ou X, Blount P, Hoffman RJ, Kung C. One face of a transmembrane helix is crucial in mechanosensitive channel gating. Proc Natl Acad Sci USA. 1998; 95:11471–11475. [PubMed: 9736761]
36. Perozo E, Cortes DM, Sompornpisut P, Kloda A, Martinac B. Open channel structure of MscL and the gating mechanism of mechanosensitive channels. Nature. 2002; 418:942–948. [PubMed: 12198539]
37. Saint N, Lacapere JJ, Gu LQ, Ghazi A, Martinac B, Rigaud JL. A hexameric transmembrane pore revealed by two-dimensional crystallization of the large mechanosensitive ion channel (MscL) of *Escherichia coli*. J Biol Chem. 1998; 273:14667–14670. [PubMed: 9614061]
38. Schrempf H, Schmidt O, Kummerlen R, Hinnah S, Muller D, Betzler M, Steinkamp T, Wagner R. A prokaryotic potassium ion channel with two predicted transmembrane segments from *Streptomyces lividans*. EMBO journal. 1995; 14:5170–5178. [PubMed: 7489706]
39. Spencer RH, Chang G, Rees DC. ‘Feeling the pressure’: structural insights into a gated mechanosensitive channel. Curr Opin Struct Biol. 1999; 9:448–454. [PubMed: 10449367]
40. Steinbacher S, Bass R, Strop P, Rees DC. Structures of the prokaryotic mechanosensitive channels MscL and MscS. Curr Top Membr. 2007; 58:1–24.
41. Sukharev S, Betanzos M, Chiang CS, Guy HR. The gating mechanism of the large mechanosensitive channel MscL. Nature. 2001; 409:720–724. [PubMed: 11217861]
42. Sukharev S, Durell SR, Guy HR. Structural models of the MscL gating mechanism. Biophys J. 2001; 81:917–936. [PubMed: 11463635]
43. Sukharev SI, Martinac B, Arshavsky VY, Kung C. Two types of mechanosensitive channels in the *Escherichia coli* cell envelope: solubilization and functional reconstitution. Biophysical J. 1993; 65:177–183.
44. Sukharev SI, Blount P, Martinac B, Blattner FR, Kung C. A large-conductance mechanosensitive channel in *E. coli* encoded by mscL alone. Nature. 1994; 368:265–268. [PubMed: 7511799]
45. Sukharev SI, Blount P, Martinac B, Kung C. Mechanosensitive channels of *Escherichia coli:* the MscL gene, protein, and activities. Ann Rev Physiol. 1997; 59:633–657. [PubMed: 9074781]
46. Sukharev SI, Schroeder MJ, McCaslin DR. Stoichiometry of the large conductance bacterial mechanosensitive channel of *E. coli.* A biochemical study. J Memb Biol. 1999; 171:183–193.
47. Sukharev SI, Sigurdson WJ, Kung C, Sachs F. Energetic and spatial parameters for gating of the bacterial large conductance mechanosensitive channel, MscL. J Gen Physiol. 1999; 113:525–540. [PubMed: 10102934]
48. van den Bogaart G, Krasnikov V, Poolman B. Dual-color fluorescence-burst analysis to probe protein efflux through the mechanosensitive channel MscL. Biophys J. 2007; 92:1233–1240. [PubMed: 17142294]
49. Walton TA, Rees DC. Structure and stability of the C-terminal helical bundle of the *E. coli* mechanosensitive channel of large conductance. Protein Sci. 2013; 22:1592–1601. [PubMed: 24038743]
50. Wang LC, Morgan LK, Godakumbura P, Kenney LJ, Anand GS. The inner membrane histidine kinase EnvZ senses osmolality via helix-coil transitions in the cytoplasm. EMBO J. 2012; 31:2648–2659. [PubMed: 22543870]
51. Wang Y, Liu Y, Deberg HA, Nomura T, Hoffman MT, Rohde PR, Schulten K, Martinac B, Selvin PR. Single molecule FRET reveals pore size and opening mechanism of a mechano-sensitive ion channel. eLife. 2014; 3:e01834. [PubMed: 24550255]
52. Yang LM, Wray R, Parker J, Wilson D, Duran RS, Blount P. Three routes to modulate the pore size of the MscL channel/nanovalve. ACS nano. 2012; 6:1134–1141. [PubMed: 22206349]

53. Yoshimura K, Usukura J, Sokabe M. Gating-associated conformational changes in the mechanosensitive channel MscL. Proc Natl Acad Sci USA. 2008; 105:4033–4038. d. [PubMed: 18310324]

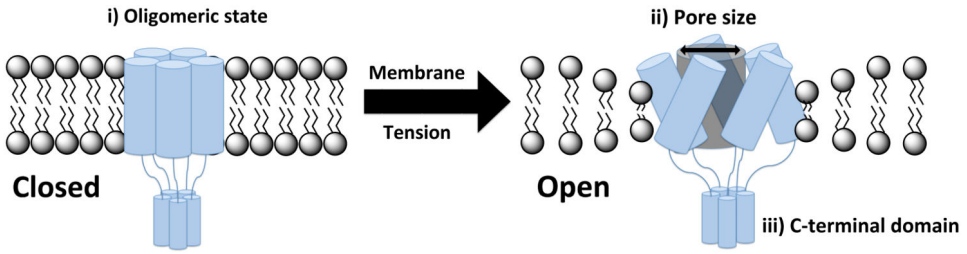

Figure 1. Schematic representation of tension dependent gating of the mechanosensitive channel MscL

The equilibrium between the closed and open forms of MscL is sensitive to membrane tension, with tension stabilizing the open conformation with the greater cross-sectional area. Features of MscL highlighted in this review that influence the response of this channel to applied tension and the conductance properties of the open state include the (i) oligomeric state, (ii) pore size and (iii) C-terminal domain.

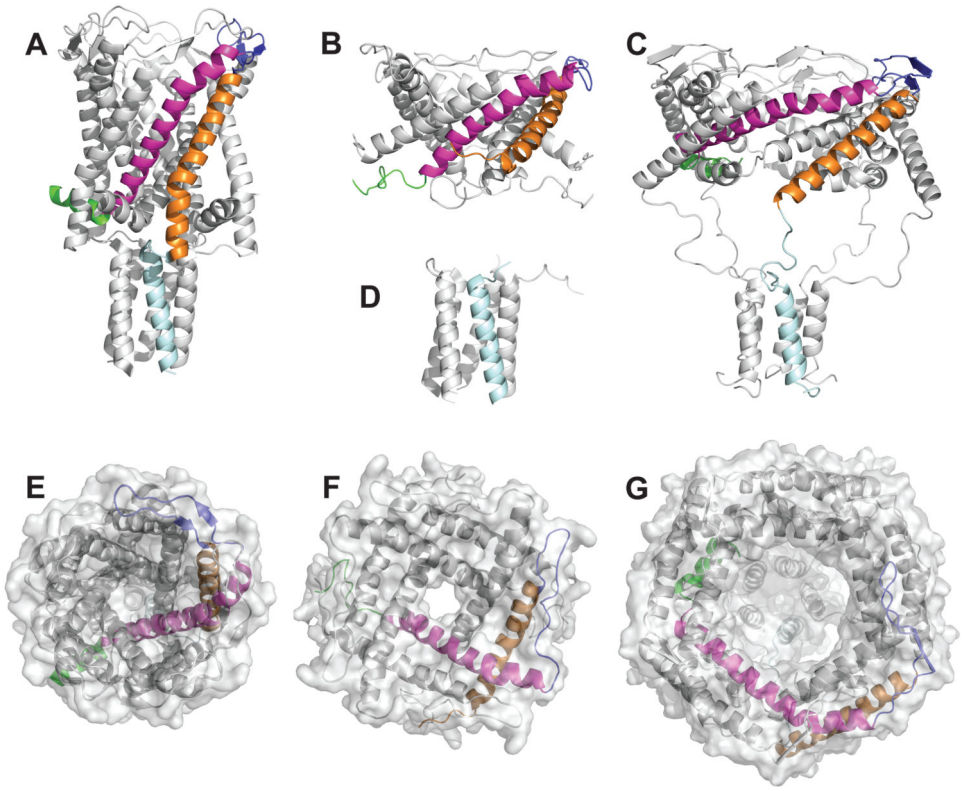

Figure 2. Crystallographic and *in silico* Models of MscL

Secondary structural elements of a monomer are labeled with the following scheme: N-terminal helix (green), TM1 (magenta), periplasmic loop (blue), TM2 (orange), C-terminal helix (light cyan). **a,e** Side and top views of the MtMscL (PDBID: 2OAR) crystallographic structure represented as a ribbon diagram. [10,40] **b,f** Side and top views of the SaMscL (CΔ26) (PDBID: 3HZQ) crystallographic structure represented as a ribbon diagram. [28] **c,g** Side and top views of the Sukharev and Guy [42] open state EcMscL model. **d** Side view of the EcMscL-CTD crystallographic structure (PDBID: 4LKU) [48]. **e,f,g** Surface rendering of the top views for a, b, c, illustrating the respective pore sizes of each model.

Table 1
Comparative Summary of Bacterial Channel Properties

Comparison of selected channel properties for bacterial channels KscA, OmpF, MscS and MscL.

Channel	Ion-Selectivity	Conductance (nS)	Mechanosensitivity
KcsA[26,38]	K^+	0.1	none
OmpF[3,13]	Slight cation selectivity	0.3 (single pore)	none
MscS[27]	Slight anion selectivity	1	5-8 mN m^{-1}
MscL[44]	Non-selective	3	10-12 mN m^{-1}

Table 2

Reported oligomeric states of four MscL homologues

Oligomeric states of detergent solubilized protein observed using various techniques are indicated with referenced studies in brackets.

	Cross-linking	Crystallography	SEC-MALS	AUC	OCAM[17]
EcMscL	1[20],5[46],6[6]	--	6[17]	5[46]	5,6 (mix)
MtMscL	5[10]	5[10,40]	5[17]	--	5
SaMscL	4[15,28],5[15]	--	4[15],5[15,17]	4[15],5[15]	5
SaMscL(CΔ26)	4[23,28], 5[23]	4[28]	4[15,17]	--	4,5 (mix)